Exploring LULC changes in Pakhal Lake area, Telangana, India using QGIS MOLUSCE plugin

Article *in* Spatial Information Research · February 2023

DOI: 10.1007/s41324-023-00509-1

CITATIONS
43

READS
1,838

3 authors:

Ashok Amgoth
National Institute of Technology Warangal
4 PUBLICATIONS **191** CITATIONS
SEE PROFILE

H. P. Rani
National Institute of Technology Warangal
76 PUBLICATIONS **1,106** CITATIONS
SEE PROFILE

Jayakumar Kv
Indian Institute of Technology Dharwad
75 PUBLICATIONS **855** CITATIONS
SEE PROFILE

Spatial Information Research
https://doi.org/10.1007/s41324-023-00509-1

Exploring LULC changes in Pakhal Lake area, Telangana, India using QGIS MOLUSCE plugin

Ashok Amgoth[1] · Hari Ponnamma Rani[2] · K. V. Jayakumar[3]

Received: 26 September 2022 / Revised: 20 January 2023 / Accepted: 20 January 2023

Abstract
Dynamic processes such as environmental, economic, and social factors influence land use and land cover (LULC) changes, with temporal and spatial variations. This study aims to identify changes in LULC and predict future trends in the Pakhal Lake area in Peninsular India. Satellite images for the years from 2016 to 2022 were used for LULC classification using deep learning with Sentinel −2 imagery in Google Earth Engine (GEE). Dynamic World dataset is used to classify the LULC changes of the study area with a 10 m near-real-time dataset. Images were classified based on six different LULC classes, namely water, vegetation, flooded vegetation, agriculture, built-up area, and bare land. The Cellular Automata–Artificial Neural Network (CA−ANN) technique was used to predict LULC changes. QGIS plugin MOLUSCE with Multi-Layer Perception (MLP), was used to predict and determine potential LULC changes for 2025 and 2028. The overall Kappa coefficient value of 0.78, and an accuracy of 82% indicated good results for LULC changes and projected maps for 2025. Prediction of LULC changes using MLP−ANN for the years 2025 and 2028 showed increase in agriculture, built-up areas, and barren land. The results of the study will be useful to develop better management techniques of natural resources.

Keywords Land use and land cover · Image classification · GEE · Predicted LULC · Multilayer Perceptron MLP−ANN · QGIS

1 Introduction

Most countries confront challenges due to rapid and unplanned urbanization, while developed and industrialized countries confront fewer difficulties than the less industrialized countries [1]. Land cover consists of vegetation, hydrological, geological, and man-made features and structures. Based on most land cover classifications, an area of a defined size falls into one of several categories. Before the knowledge of satellite images, the creation of maps and the classification of land cover relied on geodetic surveying. Thus, land cover data representing the landscape before the satellite era were usually based on digitized maps at a scale of 1:100,000 or finer. By studying the past LULC changes, it is possible to model to predict the LULC trends over a given time period. Such study will provide scientific planning and effective management, as well as guiding regional socio-economic development. Consequently, accurate information on land cover changes is required to understand and assess the LULC changes.

Human actions are causing unprecedented changes in the Earth's environment at varying rates, magnitudes, and spatial scales [2]. Significant LULC changes reflect the increase in the rate of urban expansion in recent decades, due to rapid population migrations from rural areas to urban for improved economic conditions [3]. The dynamics of land use due to population change need to be monitored [4]. The detection of LULC change is critical for understanding

✉ Ashok Amgoth
ashoka6@student.nitw.ac.in

Hari Ponnamma Rani
hprani@nitw.ac.in

K. V. Jayakumar
kvj@nitw.ac.in

[1] Research Scholar, Department of Civil Engineering, National Institute of Technology, Warangal, India

[2] Department of Mathematics, National Institute of Technology, Warangal, India

[3] Department of Civil Engineering, National Institute of Technology, Warangal, India

the landscape dynamics over a known time period with sustainable management measures [5]. Different strategies for LULC change detection analysis are available in the literature [6]. Remote Sensing (RS) and GIS are critical tools that can be used to collect reliable and timely spatial data on LULC, and to assess variations in the study area [7–9].

LULC changes can be forecast and analyzed to understand global interactions, forest decentralization, biodiversity damage, and future management strategies [10]. As a result of widespread change, the process of change that is primarily driven by natural phenomena and anthropogenic activities has become more rapid. Satellite imagery is used to produce thematic maps, and to predict the future LULC over time, which is also important in planning and managing the process of urbanization. The accessibility measures represent the human influence on land change processes in the LULC models [11]. LULC change can be predicted by generating a transition probability matrix over a period of time [12].

The LULC changes can be identified by considering the Markov chain (MC) and cellular automaton (CA) models. These models were developed to predict land use conversion [13]. The QGIS MOLUSCE plug-in model (Land Use Change Evaluation Module) created with the CA model allows the possible LULC changes to be estimated [14]. A transition probability matrix is included in this model. This plugin uses MLP – ANN, Weight of Evidence (WoE), and Multi-Criteria Evaluation (MCE). Land use planning and management can benefit from the accurate future LULC predictions provided by the CA – ANN in the MOLUSCE model [15]. The MOLUSCE model can be used to predict future changes in land and forest cover; to identify deforestation in vulnerable areas; to analyze temporal shifts in LULC; and to predict future land use changes [16, 17].

In this study, a machine-learning modelling of fire susceptibility in a forest–agriculture mosaic landscape in southern India is proposed. Geospatial data, machine learning, and spatial statistical tools were used to identify changes, and regions susceptible to forest fire, in Wayanad's forested terrain in the southern Western Ghats [18].

2 Methods

2.1 Study area

The study area, Pakhal (artificial) lake region, is located in Pakhal sanctuary, close to the Narsampet town of Warangal district in Telangana, India, at about latitude 17° 95″ 0′ N and longitude 79° 00″ 0′ E, as shown in Fig. 1. The lake encompasses an area of 30 km^2, and is believed to have been built in 1213 AD by the Kakatiya King, Ganapathidev. The 900 km^2 Pakhal Wildlife Sanctuary is located around the lake.

Pakhal lake region has a tropical climate throughout the year. The annual minimum and maximum temperatures vary from (15 to 45) degrees Celsius. Most inhabitants can be seen in their natural habitat during the winter months. Average precipitation in this area is 1,225 mm. During the southwest monsoon season, maximum rainfall of about 690 mm occurs in the month of August over the region. The land cover of Pakhal watershed predominantly consists of shrub and agricultural lands with both Kharif and Rabi crops. The major crops grown in this area are cotton and paddy. Other minor cultivated crops include groundnut, maize, and castor oil beans. The soil present in the watershed consists of sandy clayey loams with mixed red and black soils [19]. Figure 2 shows a few field photos of Pakhal lake.

2.2 Data and criteria

In the digital elevation model (DEM), the slope, aspect ratio, and distance are included in the dataset using Euclidean distance method for the study area. The dataset includes the LULC thematic maps for 2016, 2019, and 2022. The LULC maps were obtained from the Google Earth Engine (GEE). The road and built-up area maps are available on the OpenStreetMap website (http://www.openstreetmap.org).

Dynamic World dataset collection is used to classify the LULC changes of the study area with a 10 m near-real-time (NRT) dataset that includes class probabilities and label information using GEE. Dynamic World predictions are freely available for the Sentinel-2 L1C collection from 2015-06-27 to date. The revisit frequency of Sentinel-2 is between 2 and 5 days, depending on the latitude. Dynamic World predictions are generated for Sentinel-2 L1C images with *CLOUDY_PIXEL_PERCENTAGE* less than or equal to 35%. Predictions are masked to remove the clouds and cloud shadows using a combination of S2 Cloud Probability, Cloud Displacement Index, and Directional Distance Transform.

Table 1 provides detailed information on the sources of the datasets, while Table 2 provides a description of the LULC categories from 2016 to 2022. Modelling criteria were carefully chosen to achieve the required accuracy. For LULC studies, many researchers have considered distance from road, river, built-up area, DEM, aspect ratio, population density, and slope [20, 21]. For the three considered thematic LULC maps, DEMs, slopes, aspect ratio, and distance from the road were considered. Road distance was downloaded as a shapefile from the OpenStreetMap, and uploaded to ArcGIS 10.4. Euclidean distance is the main way to perform distance analysis, which measures the distance from each cell to the nearest source.

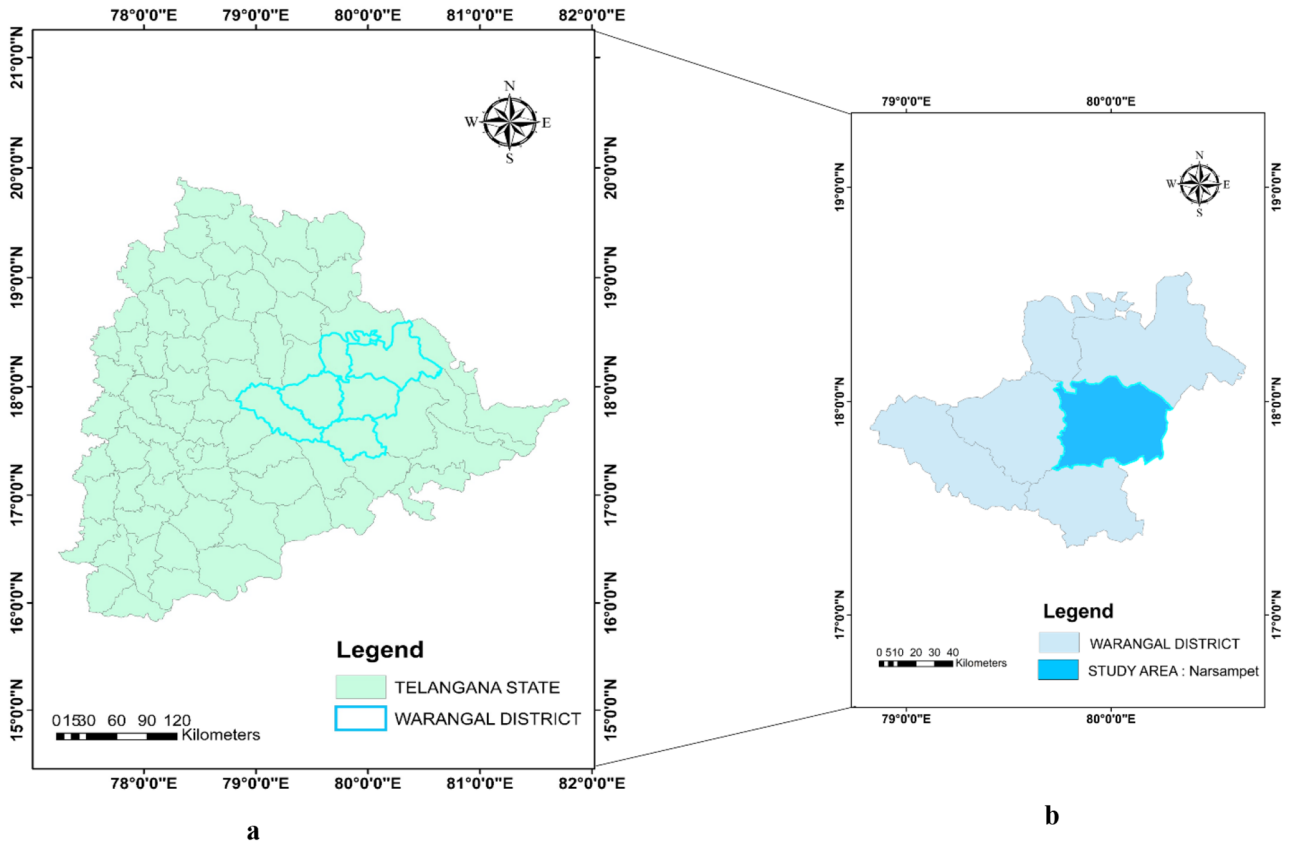

Fig. 1 The study area: Pakhal Lake area in Warangal District, Telangana, India, **a** Telangana State, **b** Warangal District showing the Narsampet Region

2.3 Methods and inputs

In the MLP–ANN learning process of the CA model (Table 2), the LULC changes characterized by the transition probabilities were used. Quantum GIS 2.18.24 with the MOLUSCE plugin was used in this approach. Six LULC prediction stages were included in the MOLUSCE plugin [21].

The LULC change maps for the initial (2016) and final (2019) years were included in the first stage of the model. A LULC change map was created using DEM, aspect ratio map, slope map, and Euclidian distance. Based on Fig. 3, the pattern of changes in the study area between 2016 and 2019 was determined. Using the same dataset, the classified LULC maps were extracted from the GEE in raster image format, which is identical to the geological coordinates of the UTM 44 N projection with an accuracy of 30 m pixel resolution.

Based on the change percentage of area over the year, the plugin MLP–ANN was used to project the LULC change. A land use map was also created, showing the changes in land use between 2016 and 2019 in six categories: water bodies, vegetation, flooded vegetation, agriculture, built-up land, and barren land. A transition matrix was created to show the pixel change between the land use coverages. To predict the future LULC maps, the current LULC patterns and dynamics were assumed to be continuous. The LULC transition map is also predicted for the years 2025 and 2028 by considering the classified raster images taken by GEE between the years 2016 and 2019.

2.4 Evaluation correlations and area change

Correlations between the two raster images were evaluated using Pearson correlation, Crammer coefficient, and joint information uncertainty [21]. The LULC changes and category of each area were then calculated between 2016 and 2019. The algorithm also generated a transition matrix showing variation of change of pixel from one type to another. The purpose of this phase was to calculate the changes in area in km^2 between the LULCs of 2016 and 2019 [16, 20].

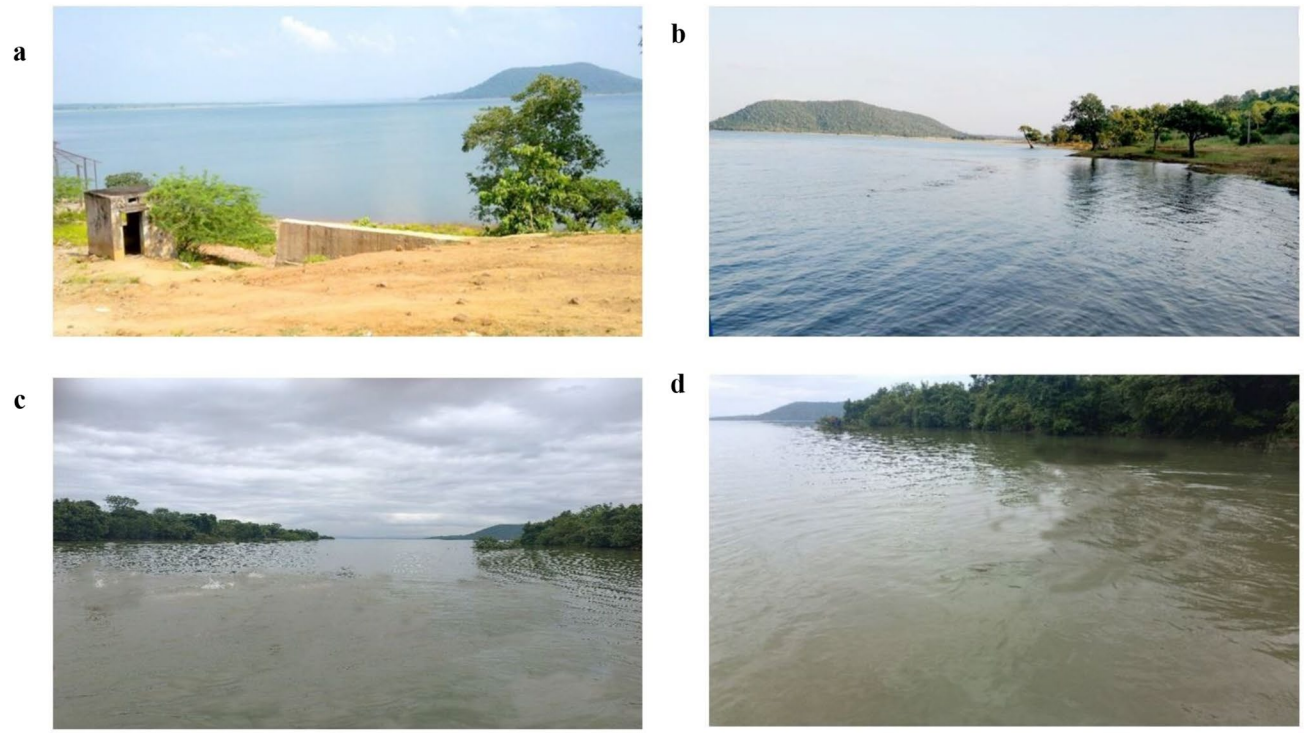

Fig. 2 Field photos of Pakhal lake wildlife sanctuary, **a** North East view, **b** South West view, **c** and **d** North West views

Table 1 Data used

Data	Criteria	Year	Description	Source	Format
DEM	Digital Elevation model, Aspect ratio, Slope	2014	30 m spatial resolution	GEE, USGS Earth Explore	.tif
Road	Distance from the road	2015	Road map	OpenStreetMap Arc GIS	.shp
LULC map	Classification	2016 2019 2022	Landsat 8 imagery 30 m resolution	Google Earth Engine (GEE)	.tif

Table 2 Change in probability matrix LULC from 2016 to 2019

Class	Water	Vegetation	Flooded vegetation	Agriculture	Built up	Bare land	Sum
Water	0.955	0.003	0.033	0.007	0.001	0.001	1
Vegetation	0.006	0.896	0.006	0.087	0.004	0.001	1
Flooded vegetation	0.215	0.040	0.681	0.061	0.002	0.001	1
Agriculture	0.021	0.123	0.028	0.817	0.010	0.001	1
Built up	0.002	0.014	0.001	0.048	0.934	0.001	1
Bare land	0.055	0.374	0.010	0.514	0.015	0.032	1
Sum	1.254	1.45	0.759	1.534	0.966	0.037	6

2.5 MLP – ANN and transition potential modelling

Although there are several methods to calculate the probabilistic transition maps, such as MLP – ANN, WoE, LR, and Multi-Criteria Evaluation (MCE), a number of approaches have been used to calibrate and simulate LULC changes statistically and regionally [22, 23]. In the present study, the plugin MLP – ANN forecasting method was used to forecast the 2022 LULC map. The Kappa coefficient (Eqs. (1)–(3)) was used to verify the accuracy of the projected LULC maps:

$$Kappa = \frac{P_0 - P_e}{1 - P_e} \tag{1}$$

where, P_e denotes the proportion of expected agreements, and P_0 denotes the proportion of actual agreements:

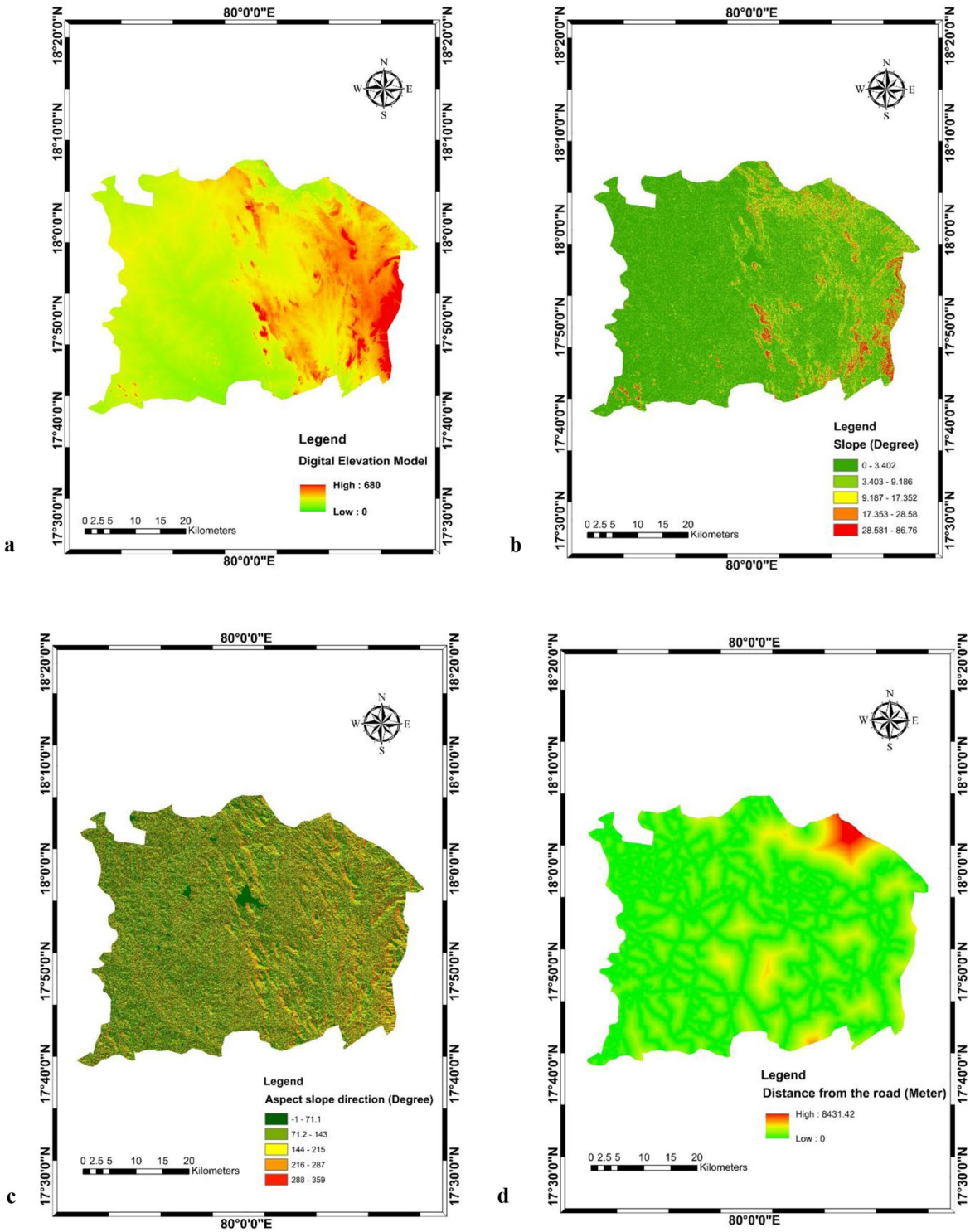

Fig. 3 Explanatory maps of the study area, **a** DEMs, **b**slope, **c** aspect ratio, **d** distance from road

$$\mathrm{P}_0 = \sum_{i=1}^{c} P_{ij} \tag{2}$$

$$\mathrm{P}_\mathrm{e} = \sum_{i=1}^{c} p_i T_p T_j \tag{3}$$

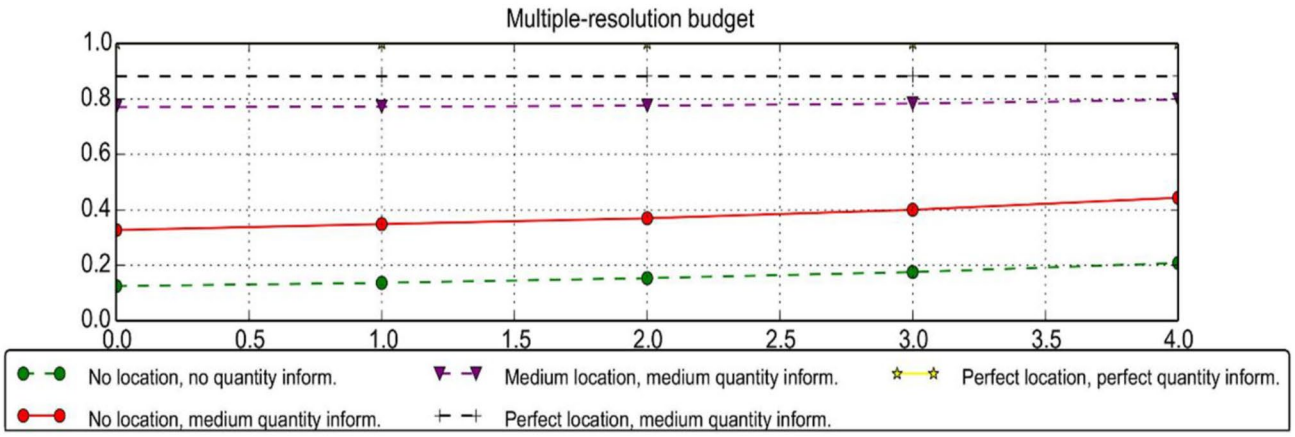

Fig. 4 Comparison of the 2022 LULC observed data with the 2022 predicted data

Table 3 Different combinations of explanatory maps and Kappa coefficients

Sl. No.	Various Spatial variable combinations	Percentage of Kappa correctness (%)	Kappa coefficient
1	DEM, Slope, Aspect ratio and Distance from Road	78.2	0.78
2	DEM, Slope	74.12	0.62
3	DEM, Aspect ratio	71.5	0.60
4	DEM, Slope, Aspect ratio	69.01	0.58

where, P_{ij} represents the i^{th} and j^{th} cells in the contingency table, T_i and T_j represent the sum of all cells in the i^{th} and j^{th} columns, respectively, and $_c$ represents the raster category count. A contingency table illustrates the relationship between the i^{th} and j^{th} cells, using a matrix that represents the variable frequency distributions. This matrix tabulates and calculates the interactions between each cell. The outcome indicates the measure of each agreed cell [17].

The LULC data and MLP – ANN were used as inputs for calibration and modeling of the LULC changes. The uncertainty of large amounts of data was difficult to implement with the algorithm. So, a continuous index of (0 to 1) was used to describe the terrain. According to the usability of the terrain, ANN determines an infinite range of (0 to 1), based on fuzzy logic. The ANN depends on the interaction between interconnected neurons, and also on the modification of mass connections between them [24]. Finally, to predict the LULC map in 2022, various parameters were determined by considering an iteration of 1,000, a momentum value of 0.06, a neighborhood of 1, a learning rate of 0.001, and a hidden layer of 10 [25, 26].

2.6 Validation

By calculating the overall Kappa coefficient, the predicted LULC maps for 2022 were validated. To forecast the 2022 LULC change map, different simulations were run using the different combinations of spatial variables. The observed and simulated LULC were validated using multi-resolution, as displayed in Fig. 4. To predict the LULC map, two to three spatial variables were combined to create the ANN – Multilayer perception, as shown in Table 3.

Table 3 discusses the overall accuracy and maximum Kappa coefficients for the various spatial variable combinations. The results found that the maximum Kappa coefficient value was 0.78, and the maximum percentage of correctness was 78.2% over the study region. The minimum Kappa coefficient value was found using the DEM, with slope and aspect as 0.58 and 69.01%, respectively, compared to other different combinations. Many researchers had considered the maximum Kappa value of 0.63 as good [15, 16, 27], and hence it can be concluded that these spatial variables have high influences in forecasting the LULC map of this study area. Then the LULC maps of 2025 and 2028 were predicted using the 2016 and 2019 LULC map with the same spatial variable combinations

3 Result and discussion

From 2016 to 2019, the elements of the probability matrix (Table 2) for the LULC categories change. In Table 2, the values range (0 to 1). The higher values indicate more significant changes, except for the diagonal cells with high values, which remain in their original category. Table 3 shows the overall accuracy and maximum Kappa coefficients for the various spatial variable combinations.

Table 4 shows the various trends of LULC changes from the year 2016 to 2022, while Table 5 depicts the analysis of LULC for every three years over the study region. Figure 5 shows the spatial variations of LULC for the years 2016, 2019, and 2022. In the year 2016, 2.76% of the total area

Table 4 LULC analysis from 2016 to 2022

Class	2016 – 2019		2019 – 2022	
	Area in km^2	% Change	Area in km^2	% Change
Water	−26.89	−1.249	26.74	1.242
Vegetation	−180.62	−8.393	17.58	0.816
Flooded vegetation	−7.19	−0.334	35.37	1.643
Agriculture	199.74	9.281	−81.58	−3.791
Built up	8.53	0.396	9.22	0.428

was covered by the water body, followed by 57% vegetation, 0.44% flooded vegetation, 36% agriculture, 2.8% built-up, and 1% bare land. The areas under the different LULC were observed to change between the years 2016, 2019, and 2022 for all the LULC classes. Compared to the year 2016, the percentage of areas covered by the water, vegetation, and flooded vegetation had decreased by (0.5, 7.5, and 0.429) %, respectively, in the year 2022. It was also observed that agriculture, built-up, and bare land areas increased by (5.5, 0.8, and 0.09) %, respectively. The percentage increases in the agriculture, built-up, and bare land were due to the increase in urbanization in the region.

For Pakhal lake, the LULC changes were found using the QGIS – MOLUSCE plugin model. The results are consistent and the percentage of correctness is 78.2%, with Kappa coefficient of 0.78. A similar plugin model was used earlier to predict the LULC change in the Bhavani basin. The percentage of correctness obtained in that study was 76.28%; thus, the present results compare well with those of the earlier study [27].

Table 6 shows the LULC changes over the classes between the years 2016 and 2025. It can be observed that the areas under agriculture, built-up, and barren land increased by (12, 0.56, and 0.43) %, respectively. But the areas covered by water, vegetation, and flooded vegetation show (− 0.342, − 8.357, and − 0.314) % decreases, respectively. The LULC changes are the percentages of the total areas. A positive value represents a positive change, while the negative values characterize the reduction of LULC area.

Table 7 illustrates the classification of land cover between 2016 and 2028. It is predicted that by 2028, the agricultural, built-up, and barren land will increase in area by (12.8, 0.58, and 0.45) %, respectively. The simulations show that the area under water, vegetation, and flooded vegetation would decrease in the year 2028, in comparison to the year 2016. With the exceptions of plantations and grassland, a decline in area is anticipated for all the other categories. Figure 5 depicts the overall LULC changes for different classes over a three-year incremental period from 2016 to 2022, while Fig. 6 shows the anticipated change in LULC between 2025 and 2028.

According to the percentage difference in LULC categories between (i) 2016 and 2025, and (ii) 2016 and 2028, the agriculture, built-up area, and barren land increased by (12, 0.5, and 0.48) %, respectively, while other categories, like water and vegetation, decreased from (2 and 8 to 10) % respectively during this time period. Note that as one class of area increases, the areas of other classes also increase, and vice versa. Future growth in the agriculture, built-up, and barren land regions suggests that the policy formulations of these study areas should prioritize these categories.

4 Conclusion

To balance conservation, competing users, and development pressures, LULC forecasts are crucial. Simulation and prediction of LULC maps for Narsampet region, Warangal district, Telangana State, India were carried out using MLP – ANN. The four spatial variable components, namely DEM, aspect ratio, slope, and distance from the road, had a significant effect on forecasting the LULC maps for the study area. In the year 2022, the Kappa coefficient calculated between the observed and predicted LULC maps had the highest score of 78.2%. Based on the same spatial variable-factor combinations used for the 2016, 2019, and 2022 LULC maps, the LULC maps for the years 2025 and 2028 were also projected. In 2025 and 2028, the estimated LULC in agriculture and built-up land showed an increase of (12 and 0.55) %, respectively. Water bodies, vegetation, and flooded vegetation are predicted to show (− 1.342, − 8.357, and − 0.314) % shrinkage in 2025, and (− 1.427, − 10.673, and − 0.429) % shrinkage in 2028, respectively. These observations show that human forces would cause the further change of forest land and other land types to built-up land and agriculture regions. To enhance their

Table 5 LULC analysis for every three-year block from 2016 to 2022

Class Area in km^2	2016		2019		2022	
	% Area covered	Area in km^2	% Area covered	Area in km^2	% Area covered	Area in km^2
Water	59.39	2.759	32.50	1.510	59.24	2.752
Vegetation	1,230.21	57.167	1,049.59	48.77	1,067.17	49.59
Flooded vegetation	9.57	0.444	2.383	0.110	37.75	1.754
Agriculture	790.96	36.755	990.70	46.03	909.12	42.246
Built-up	60.52	2.812	69.06	3.20	78.27	3.637
Bare land	1.29	0.060	7.72	0.358	0.40	0.018

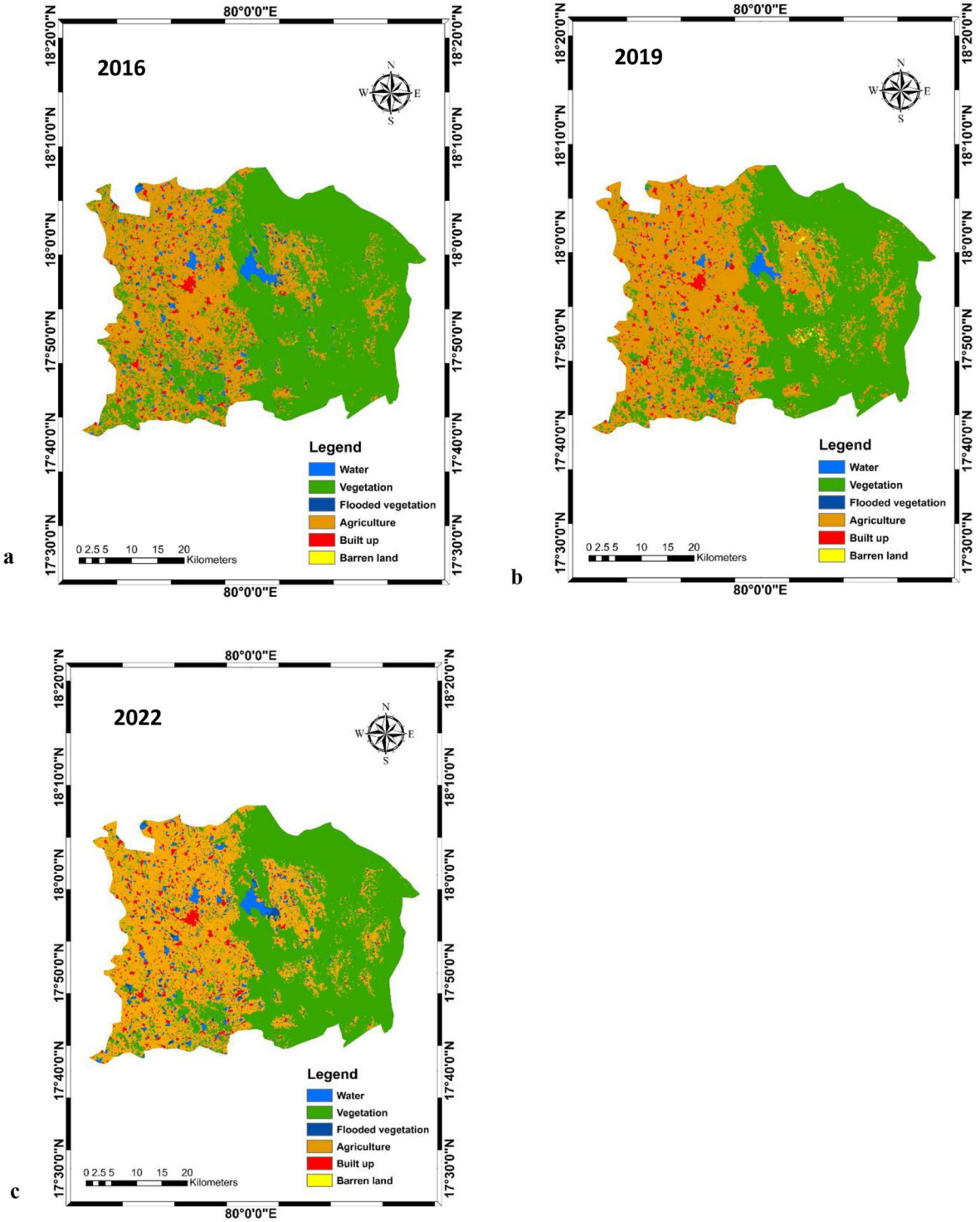

Fig. 5 Spatial variations of LULC for the years. **a** 2016, **b** 2019, **c** 2022

income, farmers typically opt to develop crops and plantations, rather than engage in reforestation. Understanding the LULC and the long-term effects it reveals, particularly the loss of forest biodiversity, is necessary in the light of this situation. To understand the potential ecological risks and biodiversity loss, the present research will help to identify LULC changes and predict the consequent land uses in the future. This research will enable farmers and decision-makers to create better management strategies and land use plans for the sustainable use of natural resources.

Table 6 Category distributions for LULCs between 2016 and 2025

Class	2016 (km^2)	2025 (km^2)	Change (km^2)	Area in % 2016	Area in % 2025	% Change 2016 – 2025
Water	59.39	30.50	−28.89	2.759	1.417	−1.342
Vegetation	1,230.21	1,050.59	−179.62	57.167	48.81	−8.357
Flooded vegetation	9.57	2.8	−6.77	0.444	0.130	−0.314
Agriculture	790.96	994.1	200.14	36.755	48.19	12.435
Built up	60.52	69.66	9.14	2.812	3.350	0.55
Bare land	1.29	2.12	0.83	0.060	0.098	0.43

Table 7 Distribution of LULC categories from 2016 to 2028

Class	2016 (km^2)	2028 (km^2)	Change (km^2)	Area in % 2016	Area in % 2028	% Change 2016 – 2028
Water	59.39	28.66	−30.73	2.759	1.331	−1.427
Vegetation	1,230.21	1,000.53	−229.68	57.167	46.494	−10.673
Flooded vegetation	9.57	0.34	−9.24	0.444	0.015	−0.429
Agriculture	790.96	1049.32	250.36	36.755	48.761	12.8
Built up	60.52	72.1	12	2.812	3.237	0.58
Bare land	1.29	3.54	2.15	0.060	0.010	0.45

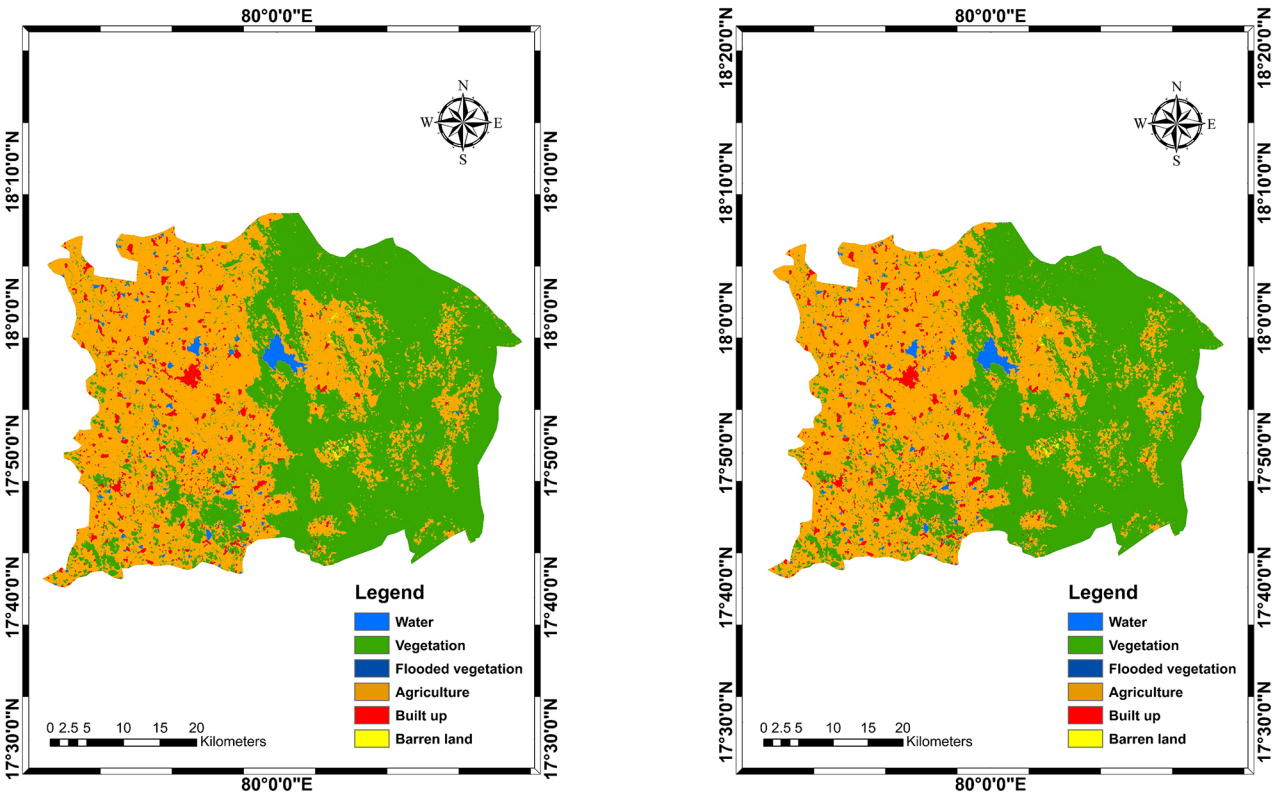

Fig. 6 Prediction of LULC for the years **a** 2025, and **b** 2028

Funding No fund was received from any source for this research, which is part of PhD research.

Declarations

Compliance with ethical standards There is no conflict of interest. On behalf of all the authors, the corresponding author claims that there is no conflict of interest.

References

1. Nurwanda, A., & Honjo, T. (2020). The prediction of city expansion and land surface temperature in Bogor City, Indonesia. *Sustainable Cities and Society*, *52*, 101772.
2. Turner, B. L. I. I., Meyer, W. B., & Skole, D. L. (1994). Global Land-Use/Land-Cover change. *Towards an Integrated Study Ambio*, *23*(1), 91–95.

3. Turner, M. G., & Ruscher, C. L. (1988). Changes in landscape patterns in Georgia, USA. *Landscape Ecology*, *1*(4), 241–251.
4. Ruiz-Luna, A., & Berlanga-Robles, C. A. (2003). Land use, land cover changes and coastal lagoon surface reduction associated with urban growth in northwest Mexico. *Landscape Ecology*, *18*(2), 159–171.
5. Rawat, J. S., & Kumar, M. (2015). Monitoring land use/cover change using remote sensing and GIS techniques: a case study of Hawalbagh block, district Almora, Uttarakhand, India. *The Egyptian Journal of Remote Sensing and Space Science*, *18*(1), 77–84.
6. Lu, D., Mausel, P., Brondizio, E., & Moran, E. (2004). Change detection techniques. *International Journal of Remote Sensing*, *25*(12), 2365–2401.
7. Reis, S. (2008). Analyzing land use/land cover changes using remote sensing and GIS in Rize, North-East Turkey. *Sensors (Basel, Switzerland)*, *8*(10), 6188–6202.
8. Pervaiz, W., Uddin, V., Khan, S. A., & Khan, J. A. (2016). Satellite-based land use mapping: comparative analysis of Landsat-8, Advanced Land Imager, and big data Hyperion imagery. *Journal of Applied Remote Sensing*, *10*(2), 026004.
9. Srivastava, P. K., Singh, S. K., Gupta, M., Thakur, J. K., & Mukherjee, S. (2013). Modeling impact of land use change trajectories on groundwater quality using remote sensing and GIS.*Environmental Engineering & Management Journal (EEMJ)*, *12*(12).
10. Dayamba, S. D., Djoudi, H., Zida, M., Sawadogo, L., & Verchot, L. (2016). Biodiversity and carbon stocks in different land use types in the Sudanian Zone of Burkina Faso, West Africa. *Agriculture Ecosystems & Environment*, *216*, 61–72.
11. Gashaw, T., Tulu, T., Argaw, M., & Worqlul, A. W. (2017). Evaluation and prediction of land use/land cover changes in the Andassa watershed, Blue Nile Basin, Ethiopia. *Environmental Systems Research*, *6*(1), 1–15.
12. Hyandye, C., & Martz, L. W. (2017). A Markovian and cellular automata land-use change predictive model of the Usangu Catchment. *International Journal of Remote Sensing*, *38*(1), 64–81.
13. Alam, N., Saha, S., Gupta, S., & Chakraborty, S. (2021). Prediction modelling of riverine landscape dynamics in the context of sustainable management of floodplain: a geospatial approach. *Annals of GIS*, *27*(3), 299–314.
14. NextGIS (2017). MOLUSCE-Quick and Convenient Analysis of Land Cover Changes.
15. Aneesha Satya, B., Shashi, M., & Deva, P. (2020). Future land use land cover scenario simulation using open source GIS for the city of Warangal, Telangana, India. *Applied Geomatics*, *12*(3), 281–290.
16. Rahman, M., Tabassum, F., Rasheduzzaman, M., Saba, H., Sarkar, L., Ferdous, J., & Zahedul Islam, A. Z. M. (2017). Temporal dynamics of land use/land cover change and its prediction using CA-ANN model for southwestern coastal Bangladesh. *Environmental Monitoring and Assessment*, *189*(11), 1–18.
17. Saputra, M. H., & Lee, H. S. (2019). Prediction of land use and land cover changes for north sumatra, indonesia, using an artificial-neural-network-based cellular automaton. *Sustainability*, *11*(11), 3024.
18. Achu, A. L., Thomas, J., Aju, C. D., Gopinath, G., Kumar, S., & Reghunath, R. (2021). Machine-learning modelling of fire susceptibility in a forest-agriculture mosaic landscape of southern India. *Ecological Informatics*, *64*, 101348.
19. Biswas, H., Raizada, A., Mandal, D., Kumar, S., Srinivas, S., & Mishra, P. K. (2015). Identification of areas vulnerable to soil erosion risk in India using GIS methods. *Solid Earth*, *6*(4), 1247–1257. https://doi.org/10.5194/se-6-1247-2015.
20. Ashaolu, E. D., Olorunfemi, J. F., & Ifabiyi, I. P. (2019). Assessing the spatio-temporal pattern of land use and land cover changes in Osun drainage basin, Nigeria. *Journal of Environmental Geography*, *12*(1–2), 41–50.
21. Hakim, A. M. Y., Baja, S., Rampisela, D. A., & Arif, S. (2019, June). Spatial dynamic prediction of landuse/landcover change (case study: tamalanrea sub-district, makassar city). In *IOP Conference Series: Earth and Environmental Science* (Vol. 280, No. 1, p. 012023). IOP Publishing.
22. Guidigan, M. L. G., Sanou, C. L., Ragatoa, D. S., Fafa, C. O., & Mishra, V. N. (2019). Assessing land use/land cover dynamic and its impact in Benin Republic using land change model and CCI-LC products. *Earth Systems and Environment*, *3*(1), 127–137.
23. El-Tantawi, A. M., Bao, A., Chang, C., & Liu, Y. (2019). Monitoring and predicting land use/cover changes in the Aksu-Tarim River Basin, Xinjiang-China (1990–2030). *Environmental Monitoring and Assessment*, *191*(8), 1–18.
24. Bhattacharya, R. K., Chatterjee, D., N., & Das, K. (2021). Land use and land cover change and its resultant erosion susceptible level: an appraisal using RUSLE and logistic regression in a tropical plateau basin of West Bengal, India. *Environment Development and Sustainability*, *23*(2), 1411–1446.
25. Das, S., & Sarkar, R. (2019). Predicting the land use and land cover change using Markov model: a catchment level analysis of the Bhagirathi-Hugli River. *Spatial Information Research*, *27*(4), 439–452.
26. Perović, V., Jakšić, D., Jaramaz, D., Koković, N., Čakmak, D., Mitrović, M., & Pavlović, P. (2018). Spatio-temporal analysis of land use/land cover change and its effects on soil erosion (case study in the Oplenac wine-producing area, Serbia). *Environmental Monitoring and Assessment*, *190*(11), 1–18.
27. Kamaraj, M., & Rangarajan, S. (2022). Predicting the future land use and land cover changes for Bhavani basin, Tamil Nadu, India, using QGIS MOLUSCE plugin. *Environmental Science and Pollution Research*, 1–12.